Interference of quantum beats in Hong–Ou–Mandel interferometry

Jing Qiu,[1] Jun-Heng Shi,[1] Yong-Sheng Zhang,[2,3] Shen-Sheng Han,[1] and You-Zhen Gui[1,4]

[1]*Key Laboratory for Quantum Optics and Center for Cold Atom Physics, Shanghai Institute of Optics and Fine Mechanics, Chinese Academy of Sciences, Shanghai 201800, China*
[2]*Lab of Quantum Information, University of Science and Technology of China, Hefei 230026, China*
[3]*e-mail: yshzhang@ustc.edu.cn*
[4]*e-mail: yzgui@siom.ac.cn*

Received December 24, 2014; revised February 20, 2015; accepted February 24, 2015; posted February 27, 2015 (Doc. ID 231297); published April 10, 2015

Quantum beats can be produced in fourth-order interference such as in a Hong–Ou–Mandel (HOM) interferometer by using photons with different frequencies. Here we present theoretically the appearance of interference of quantum beats when the HOM interferometer is combined with a Franson-type interferometer. This combination can make the interference effect of photons with different colors take place not only within the coherence time of downconverted fields but also in the region beyond that. We expect that it can provide a new method in quantum metrology, as it can realize the measurement of time intervals in three scales.

OCIS codes: (270.1670) Coherent optical effects; (270.5290) Photon statistics; (270.5570) Quantum detectors.

http://dx.doi.org/10.1364/PRJ.3.000082

1. INTRODUCTION

Interference of two photons has been widely studied because it provides important information about the optical field, such as the properties of photon statistics. Since Hong–Ou–Mandel (HOM) interferometry was first presented in 1987 [1], it has been used in many areas such as testing the violation of Bell's inequality [2,3], dispersion cancellation [4–7], quantum computing [8,9], quantum communication [7,10–12], quantum metrology [13], and quantum imaging [5,14,15].

Usually, HOM interference experiments are carried out with two incident photons at the same frequencies. However, quantum beats will arise when the two photons have different frequencies [16–20]. This information can be used to study the nondegenerate spontaneous parametric downconversion (SPDC), which is very useful for quantum communications [21–23]. In this paper we will investigate the interference effect of quantum beats when the HOM interferometer is combined with a Franson-type interferometer [24–26]. With this combination, we can show that photons with different colors can not only interfere within their coherence lengths but also interfere beyond their coherence lengths. In this case, we can realize the measurement in three scales, i.e., the coherence time of the pump photons, the coherence time of downconverted photons, and a much smaller time interval shown in the beat, which can improve the measurement sensitivity in experiments.

2. MODEL AND ANALYTICAL SOLUTION

Our proposed scheme is sketched in Fig. 1. A type II degenerate nonlinear crystal is pumped by a continuous-wave (CW) laser [27] and generates pairs of frequency anticorrelated photons, referred to as the signal and the idler. The photon pairs are sent into an HOM interferometer. In each arm, there is an unbalanced Mach–Zehnder (MZ) interferometer, so that both the signal and the idler arms are divided into two paths. Before the MZ interferometer in the signal arm, we introduce a tunable time delay τ_1 through which we can control the fourth-order interference. The lengths of the shorter (longer) paths in the signal and the idler arms have the same value when $\tau_1 = 0$. The difference between the longer path τ_2 and the shorter path τ_3 is much greater than the coherence time of the down-conversion photon pairs τ_c, i.e., τ_2–$\tau_3 \gg \tau_c$. Two filters IF1 and IF2 with different central frequencies are placed in front of detectors D1 and D2, respectively.

The biphoton state that is generated from the SPDC process can be given by [28,29]

$$|\psi\rangle = \int \mathrm{d}\omega_\mathrm{s}\mathrm{d}\omega_i \Phi(\omega_\mathrm{s},\omega_\mathrm{i})\hat{a}_s^\dagger(\omega_\mathrm{s})\hat{a}_i^\dagger(\omega_\mathrm{i})|0\rangle, \tag{1}$$

where $\Phi(\omega_\mathrm{s},\omega_\mathrm{i})$ is the biphoton spectral function, which is determined by the phase-matching conditions. As we introduce a tunable time delay τ_1 in the signal arm and an MZ interferometer in each arm, it generates a phase shift,

$$\exp(-i\omega_\mathrm{s}\tau_1)[1+\exp(-i\omega_\mathrm{s}\tau_2)][1+\exp(-i\omega_i\tau_2)], \tag{2}$$

if we assume the lengths of the shorter paths τ_3 in each arm have a value of 0. Then the biphoton state that interferes on the beam splitter should be rewritten as

$$|\psi\rangle = \int \mathrm{d}\omega_\mathrm{s}\mathrm{d}\omega_i \Phi(\omega_\mathrm{s},\omega_\mathrm{i})\exp(-i\omega_\mathrm{s}\tau_1)[1 + \exp(-i\omega_\mathrm{s}\tau_2)][1+\exp(-i\omega_i\tau_2)]\hat{a}_s^\dagger(\omega_\mathrm{s})\hat{a}_i^\dagger(\omega_\mathrm{i})|0\rangle. \tag{3}$$

The positive electrical field operators at detectors D1 and D2 are defined by

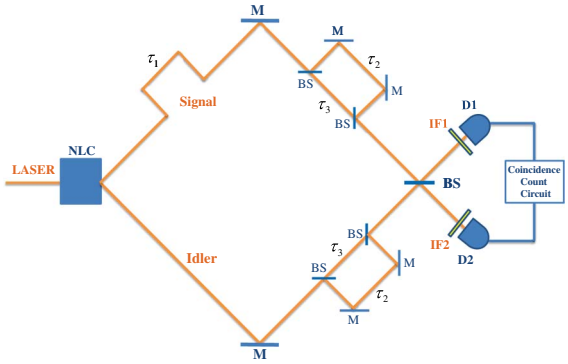

Fig. 1. Schematic diagram of the scheme. Frequency anticorrelated photon pairs are generated from the spontaneous parametric down-conversion source [nonlinear crystal (NLC)]. The signal and the idler photons are sent into an unbalanced MZ interferometer. In the signal arm, a tunable time delay τ_1 is introduced outside the MZ interferometer. Photon pairs are combined at the last beam splitter (BS), and we can observe the interference of quantum beats by observing the coincidence count rates between detectors D1 and D2. IF1 and IF2 are filters with different central frequencies set in front of the detectors. M represents the reflecting mirrors.

$$\hat{E}_1^{(+)}(t_1) = \int \mathrm{d}\omega_1 \hat{a}_1(\omega_1) g_1(\omega_1) \exp(-i\omega_1 t_1), \tag{4}$$

$$\hat{E}_2^{(+)}(t_2) = \int \mathrm{d}\omega_2 \hat{a}_2(\omega_2) g_2(\omega_2) \exp(-i\omega_2 t_2), \tag{5}$$

respectively, where $g_1(\omega_1) = \exp[-((\omega_1 - \omega_a)^2/2\sigma_1^2)]$, $g_2(\omega_2) = \exp[-((\omega_2 - \omega_b)^2/2\sigma_2^2)]$ are optical spectral functions of filters in front of detectors D1 and D2, with their central frequencies at ω_a and ω_b, respectively. For simplicity, we set the bandwidth of each filter as $\sigma_1 = \sigma_2 = \sigma$ in the following. With the state in Eq. (3) and the field operators in Eqs. (4) and (5), we can calculate the detection amplitude:

$$\begin{aligned}
&\langle 0|\hat{E}_1^{(+)}(t_1)\hat{E}_2^{(+)}(t_2)|\psi\rangle \\
&= \langle 0| \int \mathrm{d}\omega_s \mathrm{d}\omega_i \mathrm{d}\omega_1 \mathrm{d}\omega_2 \Phi(\omega_s, \omega_i) g_1(\omega_1) g_2(\omega_2) \\
&\quad \times \exp(-i\omega_1 t_1) \exp(-i\omega_2 t_2) \exp(-i\omega_s \tau_1) \\
&\quad \times [1 + \exp(-i\omega_s \tau_2)][1 + \exp(-i\omega_i \tau_2)] \\
&\quad \times \hat{a}_1(\omega_1)\hat{a}_2(\omega_2)\hat{a}_s^\dagger(\omega_s)\hat{a}_i^\dagger(\omega_i)|0\rangle.
\end{aligned} \tag{6}$$

Then the coincidence count rate between the two detectors is

$$\begin{aligned}
R(\tau_1,\tau_2) &= \int \mathrm{d}t_1 \mathrm{d}t_2 G^{(2)}(t_1,t_2) \\
&= \int \mathrm{d}t_1 \mathrm{d}t_2 |\langle 0|\hat{E}_1^{(+)}(t_1)\hat{E}_2^{(+)}(t_2)|\psi\rangle|^2 \\
&= \int \mathrm{d}\omega_s \mathrm{d}\omega_i \{\Phi(\omega_s,\omega_i)\Phi^*(\omega_s,\omega_i) - \Phi(\omega_s,\omega_i) \\
&\quad \times \Phi^*(\omega_i,\omega_s) \exp[-i(\omega_s - \omega_i)\tau_1]\}[\cos(\omega_s\tau_2) + 1] \\
&\quad \times [\cos(\omega_i\tau_2) + 1]\left\{\exp\left[-\frac{(\omega_s - \omega_a)^2}{\sigma^2}\right]\exp\left[-\frac{(\omega_i - \omega_b)^2}{\sigma^2}\right]\right. \\
&\quad \left. + \exp\left[-\frac{(\omega_i - \omega_a)^2}{\sigma^2}\right] \times \exp\left[-\frac{(\omega_s - \omega_b)^2}{\sigma^2}\right]\right\}.
\end{aligned} \tag{7}$$

For the frequency anticorrelated photon pairs, if the central frequencies of the degenerated photons are ω_0, the frequencies of the signal and idler photons are $\omega_s = \omega_0 + \omega$, $\omega_i = \omega_0 - \omega$, respectively. In this case, the biphoton spectral function $\Phi(\omega_s, \omega_i)$ can be replaced by $f(\omega) = (\sin(DL\omega/2)/DL\omega/2)$ for the type II SPDC [30,31] process, with D and L denoting the inverse group velocity difference for the biphoton and the length of the crystal, respectively. Then Eq. (7) can be rewritten as

$$\begin{aligned}
R(\tau_1,\tau_2) &= \int \mathrm{d}t_1 \mathrm{d}t_2 G^{(2)}(t_1,t_2) \\
&= \int \mathrm{d}t_1 \mathrm{d}t_2 |\langle 0|\hat{E}_1^{(+)}(t_1)\hat{E}_2^{(+)}(t_2)|\psi\rangle|^2 \\
&= \int \mathrm{d}\omega \{|f(\omega)|^2 + |f(-\omega)|^2 - [f(\omega)f^*(-\omega) \\
&\quad \times \exp(-2i\omega\tau_1) + \text{c.c.}]\}[\cos((\omega_0 + \omega)\tau_2) + 1] \\
&\quad \times [\cos((\omega_0 - \omega)\tau_2) + 1]\left\{\exp\left[-\frac{(\omega_0 + \omega - \omega_a)^2}{\sigma^2}\right]\right. \\
&\quad \times \exp\left[-\frac{(\omega_0 - \omega - \omega_b)^2}{\sigma^2}\right] + \exp\left[-\frac{(\omega_0 - \omega - \omega_a)^2}{\sigma^2}\right] \\
&\quad \left. \times \exp\left[-\frac{(\omega_0 + \omega - \omega_b)^2}{\sigma^2}\right]\right\}.
\end{aligned} \tag{8}$$

As $DL\omega \ll 1$, the analytical results can be approximately given as

$$\begin{aligned}
R(\tau_1,\tau_2) &= 1 - \exp\left(-\frac{\sigma^2\tau_1^2}{2}\right)\cos[(\omega_a - \omega_b)\tau_1] \\
&\quad - \frac{1}{2}\exp\left[-\frac{\sigma^2(\tau_1 - \tau_2)^2}{2}\right]\cos[(\omega_a - \omega_b)(\tau_1 - \tau_2)] \\
&\quad - \frac{1}{2}\exp\left[-\frac{\sigma^2(\tau_1 + \tau_2)^2}{2}\right]\cos[(\omega_a - \omega_b)(\tau_1 + \tau_2)].
\end{aligned} \tag{9}$$

3. RESULTS AND THEORETICAL EXPLANATION

We then numerically calculate the coincidence count rate with feasible experimental parameters. A CW laser with a central wavelength of 406 nm is used to pump a type II degenerate beta-barium borate crystal. In order to observe the quantum beats, the central wavelengths of two filters are set at 800 and 824 nm. The fixed time delay $\tau_2 = 6$ ps is much greater than the coherence time of the downconverted fields, which is typically 0.1–1 ps [32].

The simulated results are shown in Fig. 2. Three quantum beats emerge in different regions as we adjust the time delay τ_1 continuously. Two quantum beats with 50% visibility are seen in the two side regions, while a quantum beat with 100% visibility is seen in the middle. This result can be understood by analyzing all the different paths that the biphotons choose to take during the measurement of coincidence events between D1 and D2. There are three stages occurring along with the increased time delay:

(1) First, as illustrated in Fig. 3(a), when we scan τ_1 into the region $|\tau_1| \approx 0$ ps $\ll \tau_c$, there are two alternative paths, the longer path and the shorter path, for the photon pairs to choose to take. Besides, as biphotons arrive at the last beam splitter, we cannot tell whether the photons are both reflected or transmitted. In this sense, this interferometer is the combined form of the Franson and the HOM interferometer.

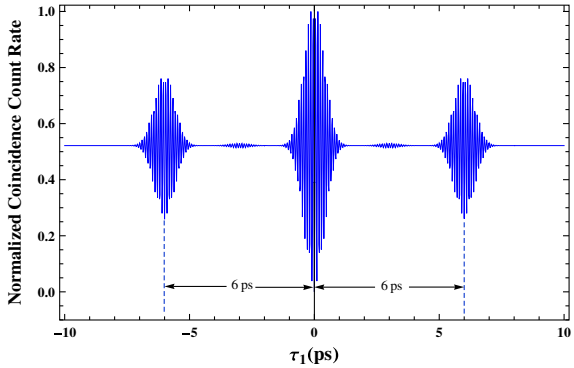

Fig. 2. Normalized coincidence count rate, which shows three quantum beats with the same interval of $\tau_2 = 6$ ps when the two filters in front of the detectors have different central frequencies. The three central dips are at the position of $\tau_1 = -6$ ps, $\tau_1 = 0$ ps, and $\tau_1 = 6$ ps.

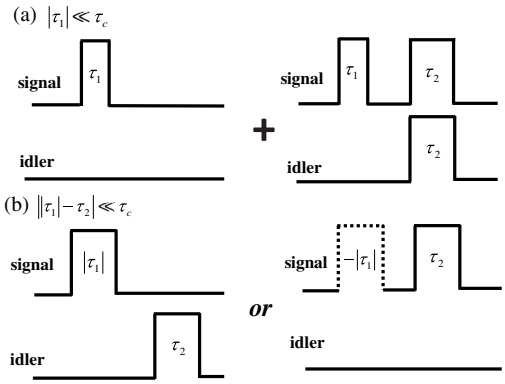

Fig. 3. Feynman's path diagrams in different regions of τ_1. (a) $|\tau_1| \approx 0$ ps $\ll \tau_c$, where each photon has two alternatives before arriving at the beam splitter; (b) $||\tau_1| - \tau_2| \approx 0$ ps $\ll \tau_c$, where each photon only has one choice before arriving at the beam splitter in order to produce interference.

A quantum beat arises whether the photon pairs choose the longer path or the shorter one. As we cannot distinguish which paths the photon pairs choose to follow, quantum beats interfere with each other with 100% visibility.

(2) Second, as shown in Fig. 3(b), when $|\tau_1|$ is increased to $|\tau_1| \approx \tau_2 = 6$ ps, quantum beats arise under the condition where the signal photons choose the shorter path while the idler photons choose the longer one when $\tau_1 = 6$ ps, and the signal photons choose the longer path while the idler photons choose the shorter one when $\tau_1 = -6$ ps. At this time, interference occurs, albeit with 50% visibility, at the positions $\tau_1 = 6$ ps and $\tau_1 = -6$ ps, because of the presence of the possibility that the idler photons take the other path, i.e., the idler photons take the shorter path when $\tau_1 = 6$ ps and the longer path when $\tau_1 = -6$ ps, which leads to a background coincidence rate independent of τ_1.

(3) Lastly, when $|\tau_1|$ reaches the region of $|\tau_1| \gg \tau_2$, photon pairs arriving at the beam splitter can be distinguished, and no interferences take place.

It should be noted that the interval τ_2 is only limited by the coherence time of the pump field.

4. DISCUSSION AND CONCLUSION

From what we have described above, we find that the three interference fringes in Fig. 2 are caused by both the HOM and the Franson-type interference; this indicates that although photons with different colors are distinguishable, the interference effect can also take place in the region far beyond the coherence time of the downconverted fields through the combination of these two kinds of interferometers. If we set limitations on the bandwidth of the downconverted field, the longer the coherence time of the pump laser is, the broader the middle envelope will be. If the coherence time of the single photon is long enough, the middle envelope will cover the other two envelopes. So through the quantum beats generated in the combined form of the HOM and the Franson-type interferometer, we can realize the measurement of time intervals on the scale of coherence time of the pump field, which is far beyond the single photon's coherence time determined by the band filters, and improve the measurement sensitivity via the beats, which could be measured according to the frequency difference of the two photons.

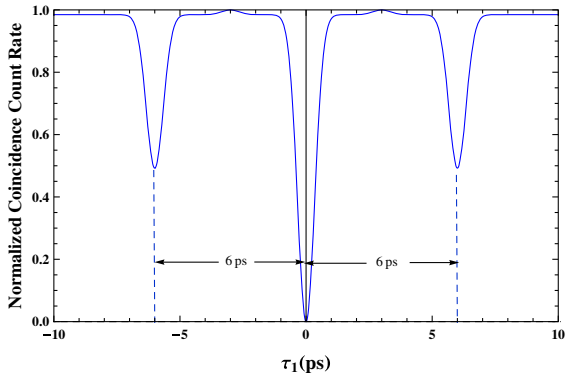

Fig. 4. Normalized coincidence count rate when the two filters have the same central frequencies. It shows three dips with the same interval of $\tau_2 = 6$ ps. The three central dips are at the positions of $\tau_1 = -6$ ps, $\tau_1 = 0$ ps, and $\tau_1 = 6$ ps.

Moreover, for comparison, in Fig. 4 we also show the simulated result in the situation where the two filters in front of the two detectors have the same central frequencies. The three dips shown in the normalized coincidence count rate are spaced by the same interval of $\tau_2 = 6$ ps and located around $\tau_1 = -6$ ps, $\tau_1 = 0$ ps, and $\tau_1 = 6$ ps. In addition, it should be noted that if the tunable time delay in this scheme is moved into one of the longer paths, i.e., the shorter paths of the two MZ interferometers are of equal value, one longer path is fixed, and the other longer path becomes tunable, the interference fringes will be very complex and both second- and fourth-order interference effects will emerge [33].

In conclusion, we have demonstrated a new scheme in which we can observe the interference of quantum beats when we combine the Franson-type interferometer with the HOM interferometer. Usually we discuss the interference effect of photons with different colors in the HOM interferometer within the coherence time of downconverted photons, but with the combination of the Franson and the HOM interferometer we can realize interference effects in the region far beyond the coherence time of the downconverted fields. Moreover, we can also realize the measurements of time intervals in the three scales shown above.

ACKNOWLEDGMENTS

This work was funded by the National Natural Science Foundation of China (Grant Nos. 10974192 and 61275122).

REFERENCES

1. C. K. Hong, Z. Y. Ou, and L. Mandel, "Measurement of subpicosecond time intervals between two photons by interference," Phys. Rev. Lett. **59**, 2044–2046 (1987).
2. Z. Y. Ou and L. Mandel, "Violation of Bell's inequality and classical probability in a two-photon correlation experiment," Phys. Rev. Lett. **61**, 50–53 (1988).
3. D. Cavalcanti, N. Brunner, P. Skrzypczyk, A. Salles, and V. Scarani, "Large violation of Bell inequalities using both particle and wave measurements," Phys. Rev. A **84**, 022105 (2011).
4. A. M. Steinberg, P. G. Kwiat, and R. Y. Chiao, "Dispersion cancellation and high-resolution time measurements in a fourth-order optical interferometer," Phys. Rev. A **45**, 6659–6665 (1992).
5. K. Cho and J. Noh, "Temporal ghost imaging of a time object, dispersion cancelation, and nonlocal time lens with bi-photon state," Opt. Commun. **285**, 1275–1282 (2012).
6. O. Minaeva, C. Bonato, B. E. A. Saleh, D. S. Simon, and A. V. Sergienko, "Odd- and even-order dispersion cancellation in quantum interferometry," Phys. Rev. Lett. **102**, 100504 (2009).
7. S. F. Pereira, Z. Y. Ou, and H. J. Kimble, "Quantum communication with correlated nonclassical states," Phys. Rev. A **62**, 042311 (2000).
8. P. C. Humphreys, B. J. Metcalf, J. B. Spring, M. Moore, X. M. Jin, M. Barbieri, W. S. Kolthammer, and I. A. Walmsley, "Linear optical quantum computing in a single spatial mode," Phys. Rev. Lett. **111**, 150501 (2013).
9. X. D. Cai, C. Weedbrook, Z. E. Su, M. C. Chen, M. Gu, M. J. Zhu, L. Li, N. L. Liu, C. Y. Lu, and J. W. Pan, "Experimental quantum computing to solve systems of linear equations," Phys. Rev. Lett. **110**, 230501 (2013).
10. E. B. Flagg, S. V. Polyakov, T. Thomay, and G. S. Solomon, "Dynamics of nonclassical light from a single solid-state quantum emitter," Phys. Rev. Lett. **109**, 163601 (2012).
11. J. Zhang, D. L. Matthias, and M. C. Carlton, "Mixing nonclassical pure states in a linear-optical network almost always generates modal entanglement," Phys. Rev. A **88**, 044301 (2013).
12. A. Rubenok, J. A. Slater, P. Chan, I. Lucio-Martinez, and W. Tittel, "Real-world two-photon interference and proof-of-principle quantum key distribution immune to detector attacks," Phys. Rev. Lett. **111**, 130501 (2013).
13. B. Bell, S. Kannan, A. McMillan, A. S. Clark, W. J. Wadsworth, and J. G. Rarity, "Multicolor quantum metrology with entangled photons," Phys. Rev. Lett. **111**, 093603 (2013).
14. A. F. Abouraddy, B. E. A. Saleh, A. V. Sergienko, and M. C. Teich, "Role of entanglement in two-photon imaging," Phys. Rev. Lett. **87**, 123602 (2001).
15. A. Gatti, E. Brambilla, L. Caspani, O. Jedrkiewicz, and L. A. Lugiato, "Quantum imaging and spatio-temporal correlations," Opt. Spectrosc. **111**, 505–509 (2011).
16. A. Pietzsch, Y.-P. Sun, F. Hennies, Z. Rinkevicius, H. O. Karlsson, T. Schmitt, V. N. Strocov, J. Andersson, B. Kennedy, J. Schlappa, A. Föhlisch, J.-E. Rubensson, and F. Gelmukhanov, "Spatial quantum beats in vibrational resonant inelastic soft x-ray scattering at dissociating states in oxygen," Phys. Rev. Lett. **106**, 153004 (2011).
17. C. Liu, J. F. Chen, S. C. Zhang, S. Y. Zhou, Y. H. Kim, M. M. T. Loy, G. K. L. Wong, and S. W. Du, "Two-photon interferences with degenerate and nondegenerate paired photons," Phys. Rev. A **85**, 021803 (2012).
18. T. Legero, T. Wilk, M. Hennrich, G. Rempe, and A. Kuhn, "Quantum beat of two single photons," Phys. Rev. Lett. **93**, 070503 (2004).
19. Y. H. Shih and A. V. Sergienko, "Observation of quantum beating in a simple beam-splitting experiment: two-particle entanglement in spin and space-time," Phys. Rev. A **50**, 2564–2568 (1994).
20. Z. Y. Ou and L. Mandel, "Observation of spatial quantum beating with separated photodetectors," Phys. Rev. Lett. **61**, 54–57 (1988).
21. Y. Li and T. Kobayashi, "Multi-photon entangled states from two-crystal geometry parametric down-conversion and their application in quantum teleportation," Opt. Commun. **244**, 285–289 (2005).
22. Y. H. Kim, S. P. Kulik, and Y. H. Shih, "Bell-state preparation using pulsed nondegenerate two-photon entanglement," Phys. Rev. A **63**, 060301(R) (2001).
23. S. Mori, J. S. derholm, N. Namekata, and S. Inoue, "On the distribution of 1550-nm photon pairs efficiently generated using a periodically poled lithium niobate waveguide," Opt. Commun. **264**, 156–162 (2006).
24. J. D. Franson, "Nonlocal cancellation of dispersion," Phys. Rev. A **45**, 3126–3132 (1992).
25. S. Y. Baek, Y. W. Cho, and Y. H. Kim, "Nonlocal dispersion cancellation using entangled photons," Opt. Express **17**, 19241 (2009).
26. D. V. Strekalov, T. B. Pittman, and Y. H. Shih, "What we can learn about single photons in a two-photon interference experiment," Phys. Rev. A **57**, 567–570 (1998).
27. H. Y. Zhang, J. F. Li, X. Y. Liang, H. Lin, L. H. Zheng, L. B. Su, and J. Xu, "High-power and wavelength tunable diode-pumped continuous wave Yb:SSO laser," Chin. Opt. Lett. **10**, 111404 (2012).
28. M. H. Rubin, D. N. Klyshko, Y. H. Shih, and A. V. Sergienko, "Theory of two-photon entanglement in type-II optical parametric down-conversion," Phys. Rev. A **50**, 5122–5133 (1994).
29. D. N. Klyshko, *Photons and Nonlinear Optics* (Gordon & Breach, 1988).
30. M. A. Sagioro, C. Olindo, C. H. Monken, and S. Pdua, "Time control of two-photon interference," Phys. Rev. A **69**, 053817 (2004).
31. A. Zhang, M. Li, and Y. H. Feng, "Experimentally achieve two photon entanglement on various emitting angle," Chin. Opt. Lett. **11**, 092701 (2013).
32. Z. Y. Ou, *Multi-Photon Quantum Interference* (Springer, 2007).
33. J. Qiu, Y. S. Zhang, G. Y. Xiang, S. S. Han, and Y. Z. Gui, "Unified view of the second-order and the fourth-order interferences in a single interferometer," Opt. Commun. **336**, 9–13 (2015).